J. Biochem. **141**, 9–18 (2007)
doi:10.1093/jb/mvm002

The Partially Unfolded State of β-Momorcharin Characterized with Steady-state and Time-resolved Fluorescence Studies

Yukihiro Fukunaga[1], Etsuko Nishimoto[1], Katsumi Yamashita[2], Takuhiro Otosu[1] and Shoji Yamashita[1,*]

[1]Institute of Biophysics, Faculty of Agriculture, Graduate School of Kyushu University, Higashiku, Fukuoka 812-8581, Japan; and [2]VALWAY Technology Center, NEC Soft, Ltd., Shinkiba, Koto-ku, Tokyo 136-8608, Japan

Received September 1, 2006; accepted November 2, 2006; published online December 13, 2006

The specific conformation of partially unfolded state of β-momorcharin was characterized through the steady-state and time-resolved fluorescence spectroscopic studies on a single Trp-190 which located adjacently to the active site. The content of secondary structure was retained, the binding of ANS was remarkably enhanced, and the correlation time of entire protein rotation was prolonged at the partially unfolded state formed by being equilibrated with the mild concentration of guanidine hydrochloride. The time-resolved fluorescence depolarization and excitation energy transfer analysis suggest that Trp-190 approached 2 Å closer to Tyr-70 and was hidden from the exposure to the protein surface, while the rotational correlation time and freedom of its segmental motion were shortened and enhanced, respectively. These results suggest that the transient folding/unfolding intermediate state of β-momorcharin adopt the specific conformation at the vicinity of the active site, although it exhibits very similar properties with those of the generally known molten-globule state.

Key words: energy transfer, folding/unfolding, β-momorcharin, molten-globule state, segmental motion of protein, time-resolved fluorescence.

Abbreviations: ANS, 1,8-anilinophthalene sulfonate; CD, circular dichroism; Gdn, guanidine hydrochloride; MG, molten-globule; RIPs, ribosome-inactivating proteins; TCSPC, time-correlated single photon counting.

Since Anfinsen's dogma that a specific three-dimensional protein structure is predominantly determined by the amino acid sequences, the studies on the protein folding/unfolding processes and mechanism are a central theme of protein science (*1, 2*). Many simple and homogeneous proteins exhibit spontaneous folding/unfolding and their folding processes are described as two states, F–U, model. However, large and multi-domain proteins adopt a conformational state, generally known as molten-globule (MG) state, during the folding/unfolding process. Even small protein, such as α-lactalbumin, equine and canine milk lysozymes, form an equilibrium partially unfolded state in the presence of chemical denaturant (*3–9*). The structure of native globular protein is stabilized by many physical forces of different natures. Hydrogen bonds determine the formation of secondary structure and hydrophobic interactions are responsible for the compaction whereas electrostatic and van der Waals interactions stabilize the unique tertiary structure. Because of their different nature responding to the changes in the protein environments, some environments might turn off one conformational factor, whereas the efficiency of other force will not change or even will be enhanced under the same conditions. In such consideration, it is expected that some specific conformational states would be involved in the protein folding/unfolding processes as an intermediate state. Their conformational and thermodynamic properties would be clues to elucidating the mechanism by which specific three-dimensional structures of protein are constructed. The significant features of MG state as a folding/unfolding intermediate have been considerably cleared by using many physico-chemical methods (*5–7, 10*). However, more details are required to understand the protein folding mechanism from the points of view of the stability, and eventually the relationship between the structure and function of protein. Because, the recent analysis of the protein unfolding process using the phase diagram methods suggests that some other conformational state as well as MG state closely involved in the protein folding and unfolding (*11*).

In the present studies, we focused on a specific conformational state of β-momorcharin found in its unfolding process. Momorcharin is a family of the ribosome-inactivating proteins (RIPs) and known as the bio-protective protein since it catalyzes the adenine release reaction of ribosomal RNA to prohibit the protein synthesis. The sequence of 249 amino acids and the X-ray crystallographic structure of β-momorcharin are confirmed already. The active site of β-momorcharin is composed of two Tyr, Arg and Glu residues. And a single tryptophan residue included in β-momorcharin covers up the lid for the active site (Fig. 1) (*12*). Because of such specific arrangement of the tryptophan residue, β-momorcharin is a quite interesting subject for studying the protein folding/unfolding. It is considered that the

*To whom correspondence should be addressed. Tel/Fax: +81-92-642-4425, E-mail: yamashita@brs.kyushu-u.ac.jp

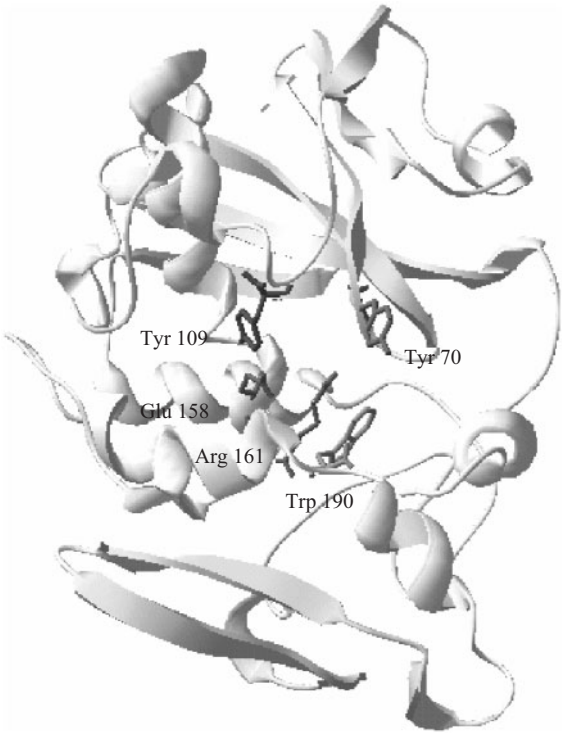

Fig. 1. **Structure of β-momorcharin.** The side chains of the amino acid residues involved in the enzyme activity are shown. The figure is based on PDB, 1CF5 (*12*).

active site of enzyme maintains the more compact conformation to complete specific roles. Besides, the tryptophan residue works as an excellent reporter for the subtle conformational change in the protein. Generally, the steady-state fluorescence spectrum has been used as a convenient tool for monitoring the protein folding/unfolding process and kinetics. But, the fluorescence spectroscopic method can provide more useful information by applying the time-resolving technique. The interactions between peptide-elements and dynamics of conformational fluctuation can be described through time-resolved fluorescence spectroscopy of tryptophan residue of which location is specified in protein (*13*). These are indispensable for characterizing the feature of the conformational states during the protein folding/unfolding process. Furthermore, the spectroscopic methods based on the Förster type resonance excitation energy transfer (FRET) and the analysis of time-resolved fluorescence depolarization would be expected to be useful to figure out the physical image of intermediate state of the protein. Since the folding/unfolding intermediate state is intrinsically disorder, we must rely on some spectroscopic methods, such as NMR, Raman, and fluorescence to investigate their conformation and dynamics. The high sensitivity and time-resolution power of fluorescence spectroscopy are best fitted to the diluted protein solution required in the protein folding/unfolding studies. In addition to these advantages, the time-resolved fluorescence depolarization is described with the orientational correlation function of transition moments fixed within the molecular plane and therefore, it is possible to specify the rotational fluctuation mode of tryptophan residue in the peptide cage and excellent time resolution power reaching to 10^{-12} s allowed us the simultaneous analysis of the segmental and the entire rotation of protein. In the present studies, we characterize the intermediate state of β-momorcharin observed during the unfolding by the chemical denaturant using the time-resolved fluorescence spectroscopy.

MATERIALS AND METHODS

Materials—Seeds of bitter gourd (*Momordica charantia*) were purchased from Nakahara Co. Ltd. Guanidine hydrochloride (Gdn), 1,8-anilinonaphthalene sulfonate (ANS), and other chemicals were of highest grade and used without further purification. Mono-S and DEAE-Sepharose used for the ion-exchange chromatography were purchased from GE Healthcare Bio-Science Corp.

Purification and Preparation of β-*Momorcharin*—The purification of β-momorcharin was performed modifying the method of Fong *et al*. (*14*). The trashed seeds of bitter gourd were ground and homogenized in 2 mM sodium phosphate buffer, pH 7.5. The resulting slurry was stirred for 5 h and centrifuged at 30,000 × g for 1 h at 4°C to extract the crude proteins. Removing the insoluble components by filtration, the crude protein solution was dialyzed against 2 mM sodium phosphate buffer, pH 7.5. The dialyzed sample was applied to a DEAE-Sepharose column equilibrated with the same buffer. The unbound proteins were collected and applied to Mono-S column equilibrated with 2 mM sodium phosphate buffer, pH 7.5. The fraction corresponding to β-momorcharin which was confirmed by the *N*-glycosidase activity against RNA was concentrated and dialyzed against 20 mM Tris–HCl buffer, pH 7.8. Every chromatography was performed on BioLogic DuoFlow system (BioRad). The purity of β-momorcharin was examined by SDS-PAGE and the gel-filtration chromatography on HPLC.

The purified β-momorcharin was prepared in 20 mM Tris–HCl buffer, pH 7.8 for unfolding experiments. Small aliquots of the sample solution were added to the reaction mixtures containing desired concentrations of Gdn. These protein solutions were incubated at 25°C for 6 h to attain the equilibrium. In these conditions, no further changes of any experimental parameters were recognized after the incubation. The concentration of β-momorcharin was determined spectrophotometrically using $OD_{280} = 1.3$ (1 mg/ml).

Steady-state and Time-resolved Fluorescence Measurements—The steady-state fluorescence emission spectra were recorded on a Hitachi 850 fluorescence spectrophotometer. The fluorescence emission spectrum was strictly corrected against the detection and excitation systems. The undesired effects of stray lights were also removed with a subtraction method. The fluorescence spectrum of ANS was measured for the protein solution including 20 μM of β-momorcharin which was equilibrated with various concentrations of Gdn. The excitation wavelengths, 297 and 380 nm were used for β-momorcharin and ANS, respectively. The steady-state fluorescence anisotropy of β-momorcharin was measured with the same instrumentation. Based on the definition,

the fluorescence anisotropy (r) was calculated after the measurements of the vertical (I_{vv}) and horizontal (I_{vh}) fluorescence intensities against the vertical excitation. The G-factor is determined by the ratio of I_{hv} to I_{hh} which were the intensities vertically and horizontally polarized components against the horizontal excitation, respectively.

The time-resolved fluorescence and fluorescence anisotropy were measured with the sub-pico second laser based time-correlated single photon counting method (TCSPC). The excitation pulse (275–300 nm) was separated from a combination of sub-picosecond Ti-Sapphire laser (Tsunami, Spectra-Physics), pulse picker with second harmonic generator (model 3980, Spectra-Physics), and third harmonic generator (GWU, Spectra-Physics). The repetition rate was 800 kHz and the obtained excitation pulse width was 100 fs. The stop pulse to drive the time to amplitude converter (TAC, 457, Ortec) was detected by a high speed APD (C5658, Hamamatsu Photonics). The fluorescence emission pulse was detected by a multi-channel plate type photomultiplier (3809U-50, Hamamatsu Photonics) and fed into TAC through a constant fraction discriminator (935, Ortec). The output signals of TAC were accumulated in 2,048 channels in a multi-channel analyzer (Maestro-32, Ortec). The channel width was 11 ps/ch.

The fluorescence decay kinetics of β-momorcharin was described with linear combination of some exponentials,

$$F(t) = \sum \alpha_i \exp\left(\frac{-t}{\tau_i}\right) \quad (1)$$

where τ_i is the fluorescence decay time of ith component and α_i is the corresponding pre-exponential factor. α_i and τ_i were determined with the iterative convolution and non-linear curve fitting methods. The adequacy of the curve-fitting was judged by the residual plots and statistic parameters, such as serial variance ratio (SVR) and sigma value (σ) (*15*).

The measurements of the fluorescence anisotropy decay were performed with the same TCSPC system. But, a Gran–Taylor polarizer was set just behind the sample to measure the decays of vertical ($I_{vv}(t)$) and horizontal ($I_{vh}(t)$) components against the vertical excitation. $I_{vv}(t)$ and $I_{vh}(t)$ were related with the fluorescence decay, $F(t)$ and anisotropy decay, $r(t)$ by the following Eqs (2) and (3).

$$I_{vv}(t) = \frac{1}{3}F(t)\{1 + 2r(t)\} \quad (2)$$

$$I_{vh}(t) = \frac{1}{3}F(t)\{1 - r(t)\} \quad (3)$$

The fluorescence anisotropy decay kinetics was given by Eq. (4),

$$r(t) = \sum \beta_i \exp\left(\frac{-t}{\phi_i}\right) \quad (4)$$

where ϕ_i is the rotational correlation time of ith component and β_i is the corresponding amplitude. The fluorescence anisotropy decay was determined by the simultaneous global analysis of $I_{vv}(t)$ and $I_{vh}(t)$ using the Eqs (1)–(4). Their adequacies were confirmed by SVR and sigma for the parallel and perpendicular, respectively. Every fluorescence measurements were performed at 25°C.

Fluorescence Quenching—The fluorescence quenching experiments were based on usual Stern-Volmer equation, $F_0/F = 1 + K_{SV}[Q]$, where F_0 and F were the fluorescence intensities in the absence and presence of the quencher molecule and K_{SV} and $[Q]$ are Stern-Volmer quenching constant and the concentration of quencher, respectively. The sample solution including 2.0 μM of β-momorcharin which was equilibrated with various concentrations of Gdn was titrated by a solution of acrylamide without changing the concentration of Gdn and protein. The fluorescence intensity was measured at the fluorescence maximum wavelength. The quenching constant K_{SV} was estimated by the slope of the Stern-Volmer plot. The collisional fluorescence quenching constant, k_q, was obtained by the average fluorescence lifetime and K_{SV}.

CD Spectrum—CD spectrum of β-momorcharin was recorded on a J-720 spectropolarimeter (JASCO). The sample solution of β-momorcharin was buffered with 20 mM Tris–HCl buffer, pH 7.8. The protein concentration used for CD spectrum was adjusted to 0.1 mg/ml. CD cuvette with 1 mm of optical-path length was used for the measurements in the far-UV region.

RESULTS

The fluorescence maximum wavelength of tryptophan residue in protein is very sensitive to the surrounding polarity. In non-polar circumstances, the fluorescence transition of Trp is attributed to ^1L_b-A and the fluorescence maximum is observed around 330 nm. When polar molecule, such as water molecules approach or the surrounding polarity is increased, the fluorescence maximum shifts to the lower energy side because of the lowering of the energy level of the fluorescence emission state by stronger dipole–dipole interactions. It is well known that the fluorescence maximum of Trp is observed around 350 nm when Trp residue is exposed to the aqueous phase 100%. This fluorescence property is a useful indicator for the conformational change in proteins. Fig. 2(A) shows the effect of Gdn on the fluorescence spectrum of β-momorcharin in 20 mM Tris–HCl buffer, pH 7.8. The fluorescence maximum of native β-momorcharin was found at 328 nm to suggest Trp residue is isolated from aqueous phase at the vicinity of the active site. The fluorescence maximum wavelength was not changed by increasing the concentration of Gdn until 2 M, although the increase in fluorescence intensity was recognized. In the presence of 5 M of Gdn, β-momorcharin gave a quite different fluorescence spectrum to suggest that β-momorcharin unfolded at this Gdn concentration. The fluorescence intensity was reduced to 25% and the maximum wavelength shifted to 355 nm.

The effects of Gdn on the fluorescence intensity, maximum wavelength, and steady-state fluorescence anisotropy of β-momorcharin are given as the functions of the concentration of Gdn in Fig. 2(B). The fluorescence

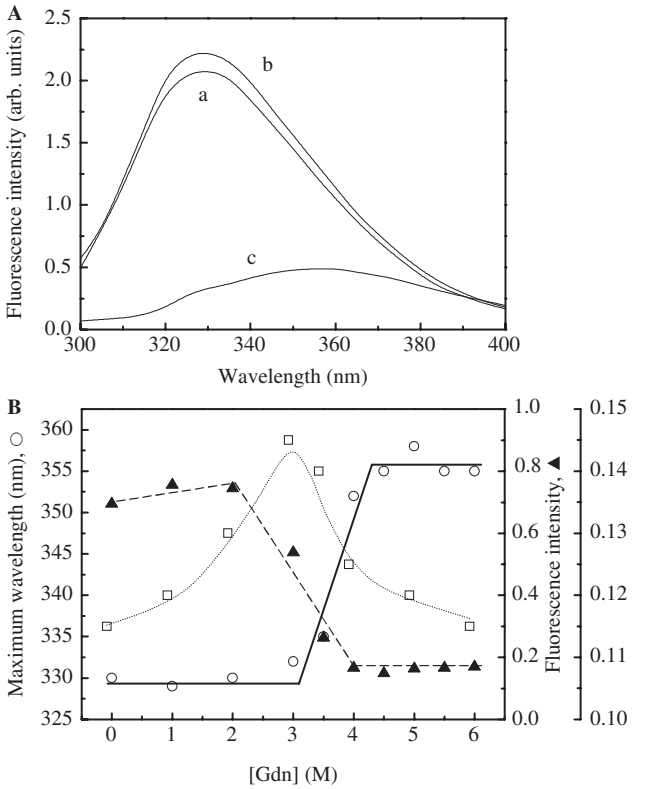

Fig. 2. **Fluorescence spectra of β-momorcharin in the buffer solution including 0 (a), 2 (b) and 5 M (c) of Gdn (A) and the Gdn concentration dependence of fluorescent spectroscopic properties of β-momorcharin (B)**. The concentration of protein was 0.08 mg/ml. ○, Fluorescence maximum wavelength; □, Steady-state fluorescence anisotropy; ▲, Fluorescence intensity. Excitation wavelength was 297 nm. The steady-state fluorescence intensity and anisotropy were measured at the fluorescence maximum wavelength.

maximum wavelength was constantly 328 nm in the lower concentration range of Gdn but it started to shift rapidly to the lower energy side at 3.5 M to reach 355 nm at 4.5 M. In the fluorescence intensity–[Gdn] curve, it was shown that the fluorescence intensity slightly increased in proportion to the concentration of Gdn but was not so much dependent on it at the concentrations lower than 2 M. At 2.5 M of Gdn, the fluorescence intensities started to decrease and reached a constant value at 4 M. The steady-state fluorescence anisotropy of β-momorcharin was lower at lower (0–2 M) and higher (4–6 M) Gdn concentration regions to give a broad maximum at about 3 M. While the fluorescence maximum and intensity give the information on the polar circumstances and interaction of tryptophan residue, the fluorescence anisotropy closely correlates with the rotational motions of tryptophan and protein itself. The increase of steady-state fluorescence anisotropy around 3 M Gdn indicates that the segmental motion of tryptophan residue would be limited and/or the hydration volume size of β-momorcharin enlarged.

The fluorescence quantum yield of 1,8-anilinonaphthalene sulfonate (ANS) is 0.004 in water and is enormously increased to about 0.75 by binding with the hydrophobic

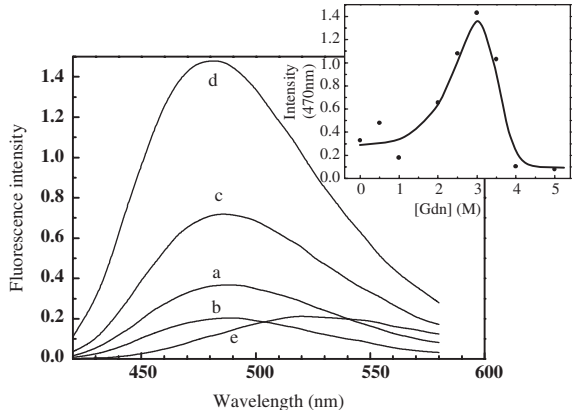

Fig. 3. **The fluorescence spectra of ANS in the solutions of β-momorcharin including 0 (a), 1 (b), 2 (c), 3 (d), and 5 M (e) of Gdn.** Insert, the fluorescence intensity of ANS vs. Gdn concentration. Excitation and emission wavelengths were 380 and 470 nm, respectively. The concentration of β-momorcharin and ANS were 2.0 and 200 μM, respectively.

pocket in protein. Using this spectroscopic property, ANS has been used for the identification and detection of partially unfolded states during the protein folding/unfolding (*16*). The binding of ANS with β-momorcharin equilibrated with various Gdn concentrations was examined through its fluorescence spectral changes. As shown in Fig. 3, the fluorescence intensity of ANS increased and then decreased with increasing the Gdn concentration to give a maximum. This result demonstrates that the hydrophobic parts of β-momorcharin are exposed to the surface to allow the access of ANS at 2–3 M of Gdn, although they are lost on the protein unfolding in the presence of Gdn higher than 4 M.

Fig. 4 shows effects of Gdn on CD spectrum of β-momorcharin. When the ellipticity at 222 nm which was the indicator for the significant presence of α-helix was plotted against Gdn concentration, it slightly decreased as the Gdn concentration increased. But, the ellipticity at far-UV region was still high at 2.5 M of Gdn to show that β-momorcharin maintains more than 90% of secondary structure. At the concentration higher than 4 M of Gdn, very small ellipticity was recognized at 217 nm.

The steady-state fluorescence and CD spectroscopic studies suggest that β-momorcharin reaches the specific conformation state in the presence of around 2–3 M Gdn between the native and unfolding states. In order to characterize the features in conformation and dynamics of this state, the time-resolved fluorescence studies were examined. Fig. 5 shows the fluorescence decay curves of β-momorcharin in the buffer solution containing 0 (a), 2 (b), and 5 M (c) of Gdn. Double or triple exponential kinetics were required to describe the fluorescence decays of β-momorcharin. The fluorescence decay parameters giving the best fits were dependent on the concentration of Gdn suggesting β-momorcharin adopted the different conformations according to the concentration of Gdn. The obtained fluorescence decay parameters are summarized in Table 1. The fluorescence decay of native β-momorcharin showed two components of which decay times were 3.56 and 0.67 ns and the pre-exponential factors were almost independent of the

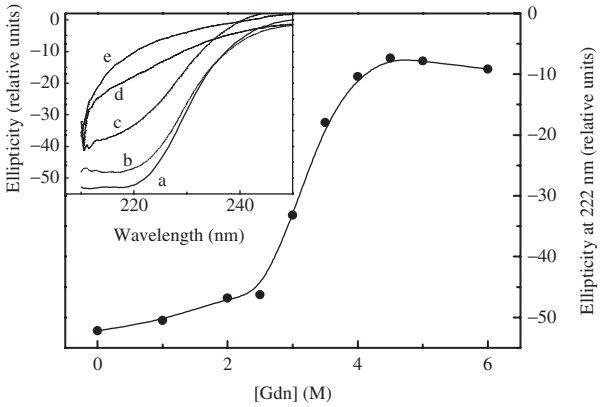

Fig. 4. **The Gdn concentration dependence of ellipticity of β-momorcharin at 222 nm.** Insert, CD spectra of β-momorcharin in the buffer solution including 0 (a), 2 (b), 3 (c), 3.5 (d), and 4 M (e) of Gdn. The concentration of β-momorcharin was 0.1 mg/ml.

emission wavelengths. The fluorescence decay properties of β-momorcharin in equilibrium with 2 M of Gdn were similar to the native one. But, it should be noted that the decay times were prolonged to 3.78 and 1.25 ns, respectively. The switch of the decay kinetics from double to triple and the reduction of average lifetime on unfolding at 5 M of Gdn demonstrates that the large scale of structural change would be induced in β-momorcharin.

Fluorescence dynamic quenching experiment of protein is used to investigate the conformational change around the tryptophan residue. Fig. 6 shows the Stern–Volmer plots of β-momorcharin in the solution including 0, 2, 3, and 5 M of Gdn. In every case, the quenching plot was so linear that Stern-Volmer constant (K_{SV}) could be estimated. The apparent quenching constant (K_{SV}) of native β-momorcharin was larger than that of the unfolded. But the accessibility of the quencher to the tryptophan residue must be evaluated by the collisional quenching constant (k_q) because the cross section of the quenching depends on the fluorescence lifetime. According to the fluorescence quenching theory, the relation between K_{SV} and k_q is given by $K_{SV} = k_q \cdot \tau_{av}$. The resulting quenching parameters are summarized in Table 2. The lower accessibility of the quencher molecule (acrylamide) to tryptophan residue in β-momorcharin was found in the solution equilibrated with 2 M of Gdn. It should be noted that the collisional quenching constant of the native β-momorcharin is 3-fold larger than that of β-momorcharin in 2 M of Gdn.

When 297 nm was used as the excitation wavelength, tryptophan residue was exclusively excited in β-momorcharin. On the excitation at 280 nm, tyrosine residue was also excited to the fluorescence state. The fluorescence decay of Trp would be independent on the excitation wavelength provided there were no Tyr works as the energy donor around Trp. On the excitation at 280 nm, the existence of rising components was recognized in the fluorescence decay profiles in the solution of β-momorcharin equilibrated with 0 and 2 M of Gdn while the unfolded β-momorcharin showed almost same decay profile regardless of the excitation

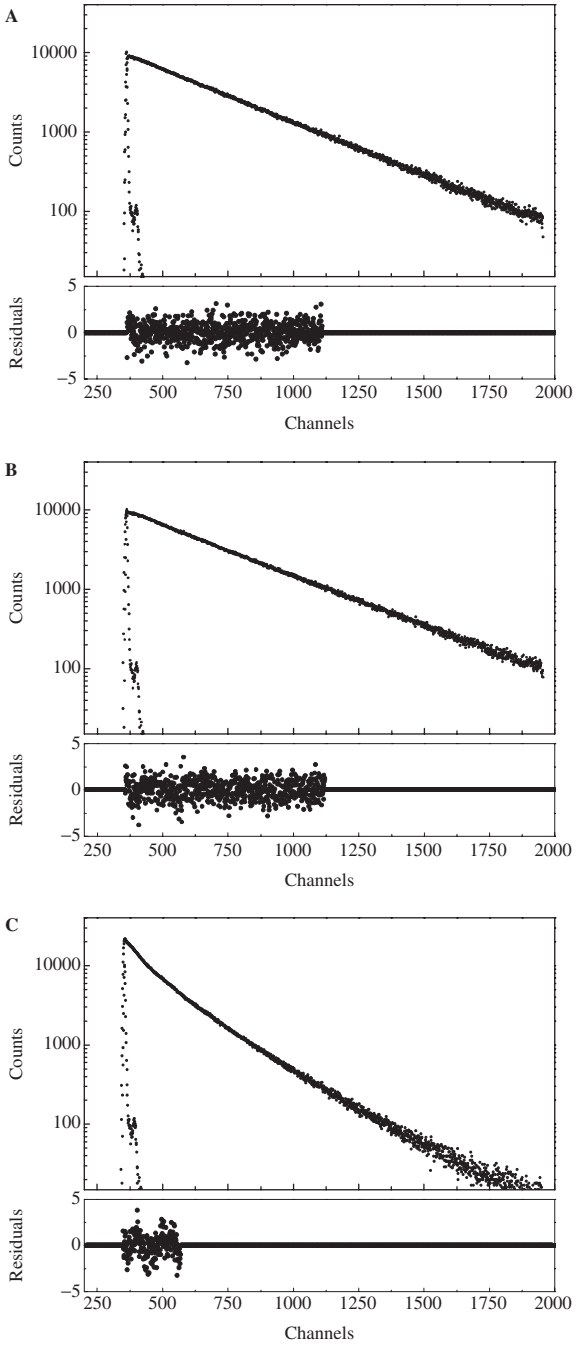

Fig. 5. **Fluorescence decay curves (upper panel) and residuals (lower panel) of β-momorcharin in the buffer solution excited at 297 nm. a, 0 M; b, 2 M; c, 5 M of Gdn.** Spike-like curves indicate the excitation pulse. Channel width was 11 ps/ch. The emission wavelengths are 330 nm (A, B) and 350 nm (C), respectively. The concentration of β-momorcharin was 0.08 mg/ml.

wavelength as shown in Fig. 7. The decay parameters giving the best fits to the fluorescence decay curves are summarized in Table 3. The negative pre-exponential factors seen in the decay kinetics of β-momorcharin suggest the excitation energy transfer from Tyr contributes to the fluorescence decay of Trp residue in the

Table 1. **Fluorescence decay parameters of β-momorcharin excited at 297 nm.**

	α_1	α_2	α_3	τ_1 (ns)	τ_2 (ns)	τ_3 (ns)	τ_{av} (ns)	σ	SVR
Native[a]	0.96	0.04	–	3.56	0.67	–	3.4	1.09	1.88
2 M Gdn[a]	0.93	0.07	–	3.78	1.25	–	3.6	1.1	1.71
5 M Gdn[b]	0.31	0.26	0.43	3.13	0.78	0.02	1.18	1.20	1.51

[a]Emission wavelength, 330 nm. [b] Emission wavelength, 350 nm.

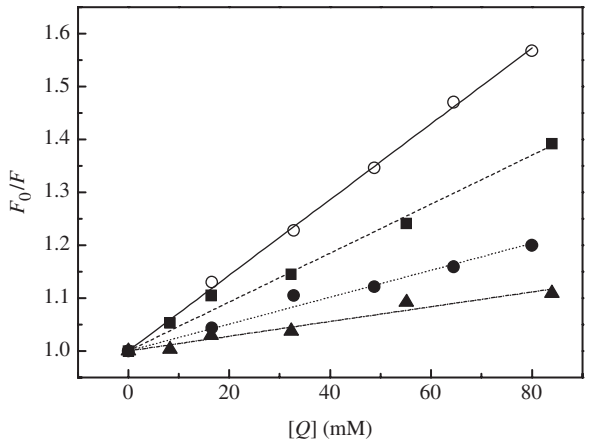

Fig. 6. **Stern–Volmer plots for the fluorescence quenching of β-momorcharin.** The fluorescence intensity ratio in the presence and absence of quencher, F_0/F was plotted against various concentration of acrylamide, [Q]. Fluorescence intensities were measured at the maximum wavelengths excited at 297 nm. ○, 0 M Gdn; ●, 2 M; ▲, 3 M; ■, 5 M. The concentration of β-momorcharin was 0.08 mg/ml.

Table 2. **Fluorescence quenching parameters of β-momorcharin by acrylamide.**

Concentration of Gdn-HCl (M)	K_{SV} (M^{-1})	τ_{av} (ns)	k_q ($M^{-1}\,ns^{-1}$)
0	7.16	3.40	2.11
2	2.54	3.60	0.71
3	1.39	2.11	0.66
5	4.63	1.18	3.92

presence of 2 M of Gdn. The decay time corresponding to the negative pre-exponential factor in the fluorescence decay of β-momorcharin in the 2 M Gdn solution was more than 2-fold shorter than that of the native state.

The time-resolved fluorescence depolarization studies provide the information on the segmental motions of Trp residue in the polypeptide cage. The fluorescence anisotropy decay curves of β-momorcharin equilibrated with 0, 2, and 5 M of Gdn are shown in Fig. 8. They are described with the double exponential kinetics. One of the two rotational correlation times is shorter and the other is longer. The longer correlation time (ϕ_2) of the native β-momorcharin was 29.3 ns as shown in Table 4. This rotational correlation time was almost consistent with the value calculated using the Einstein–Stokes relation and assuming the specific volume is 0.75 ml/mg and hydration is 0.4. Therefore, the longer rotational correlation time observed here must be attributed to one of the entire rotation of β-momorcharin. The shorter correlation time (ϕ_1) can be attributed to one for the segmental fluctuation of the peptide element including

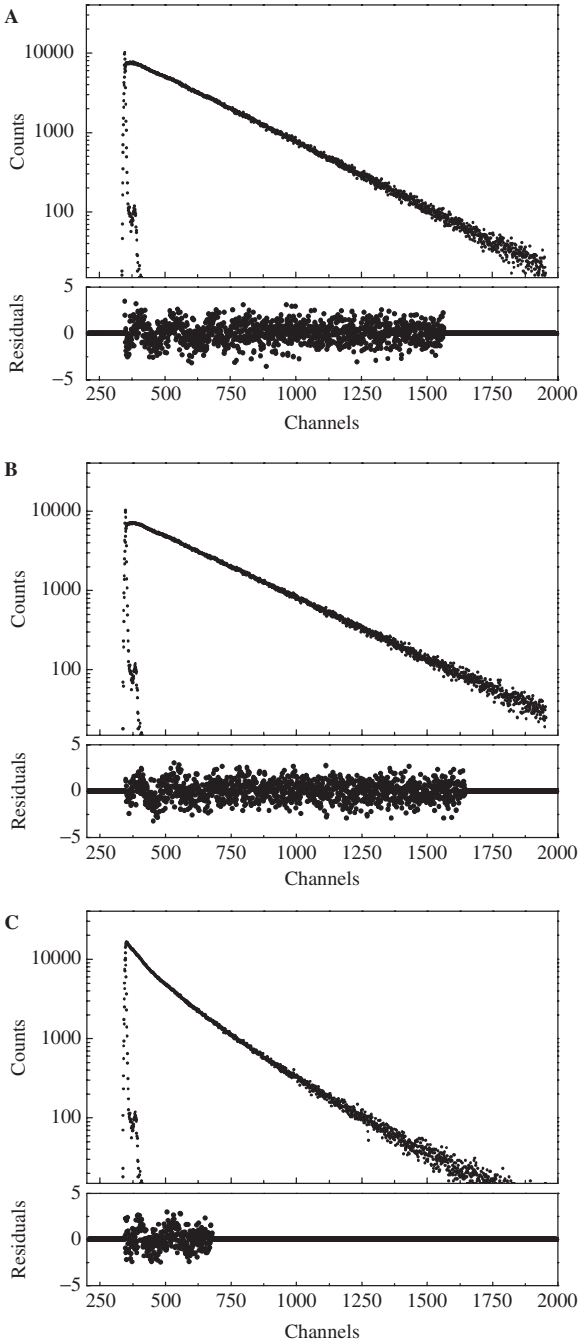

Fig. 7. **Fluorescence decay curves (upper panel) and residuals (lower panel) of β-momorcharin in the buffer solution excited at 280 nm.** a, 0 M; b, 2 M; c, 5 M of Gdn. Spike-like curves indicate the excitation pulse. Channel width was 11 ps/ch. The emission wavelengths are 330 nm (A, B) and 350 nm (C), respectively. The concentration of β-momorcharin was 0.08 mg/ml.

Table 3. **Fluorescence decay parameters of β-momorcharin excited at 280 nm.**

	α_1	α_2	α_3	τ_1 (ns)	τ_2 (ns)	τ_3 (ns)	σ	SVR
Native[a]	1.17	−0.17	–	4.17	1.45	–	1.10	1.87
2 M Gdn[a]	1.11	−0.11	–	4.51	0.63	–	1.03	1.82
3 M Gdn[a]	1.10	−0.10	–	4.24	0.68	–	1.04	1.83
5 M Gdn[b]	0.40	0.28	0.32	2.81	0.74	0.03	1.10	1.81

[a]Emission wavelength, 330 nm. [b]Emission wavelength, 350 nm.

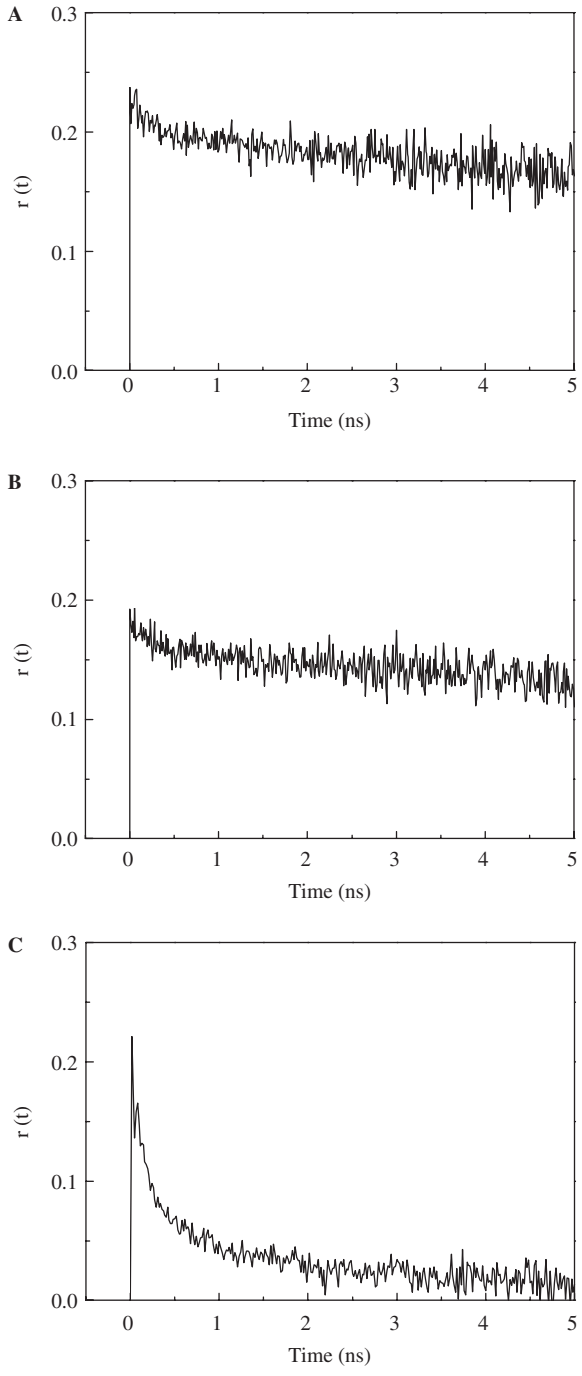

Fig. 8. **The fluorescence anisotropy decay curves of β-momorcharin in the buffer solution including 0 (a), 2 (b) and 5 M (c) of Gdn.** Excitation wavelength, 297 nm; emission wavelength, 330 nm (A, B) and 350 nm (C). The concentration of β-momorcharin was 0.08 mg/ml.

Trp residue. The results given in Table 4 suggest the hydration volume of β-momorcharin is much larger in 2 M Gdn solution. The longer correlation time (ϕ_2) of the unfolded state was considerably shorter. Probably, it would be caused by the unfolding of the protein and the corresponding correlation time would be attributed to the rotational motion of the larger peptide elements including the Trp residue. The rotational correlation time (ϕ_1) was shortened and the fractioned β_1 was also increased by increasing the Gdn concentration to 2 M. These results suggest that the segmental motion of Trp would be enhanced by the conformational change induced in the partially unfolded state of β-momorcharin.

DISCUSSION

The fluorescence intensity of Trp was decreased without shifting of the maximum wavelength at the concentration range of 2–3.5 M of Gdn and the steady-state fluorescence anisotropy shows the highest value at 3 M, while the fluorescence maximum wavelength started to shift from 328 to 355 nm at the presence of Gdn higher than 3.5 M. These steady-state fluorescence studies consistently demonstrate that β-momorcharin takes a quite different conformation from the native or unfolded state in the mild concentration of Gdn. It has been shown that some proteins such as α-chimotrypsinogen A, apomyoglobin, and α-lactalbumin formed the MG state as a transient intermediate state during the folding/unfolding process in the mild concentration of chemical denaturant or under the acidic condition. Based on the general concept, the MG states of these proteins are partially unfolded states and maintain native like secondary structures but their tertiary structures are loosened. In general, the side chain fluctuation of amino acid residues is increased on the transition from the native state to the MG state and it leads to the appearance of large hydrophobic surfaces accessible to solvent. Therefore, the fluorescence intensity of ANS is increased in the MG state. This fluorescence binding property has been used as an important criterion for the formation of the partially unfolded state of protein (*16–18*). The fluorescence of ANS was increased in the solution of β-momorcharin equilibrated with 2–3 M of Gdn where the changes of fluorescence intensity and depolarization properties due to the Trp residue were observed. The increase in the α-helix content was seen in the MG state of α-lactalbumin and some lysozymes (*19, 20*). Watanabe *et al*. (*21*) recently showed that α-helix was formed in the β-sheet region of the partially unfolded state. The co-operative interaction between the α-helices is an important factor to stabilize the folding/unfolding intermediate state. Although the

Table 4. **Fluorescence anisotropy decay parameters of β-momorcharin excited at 297 nm.**

	β_1	β_2	ϕ_1 (ns)	ϕ_2 (ns)	σ	SVR(VV)	SVR(VH)	f
Native[a]	0.03	0.16	0.53	29.3	1.06	1.98	2.03	0.16
2 M Gdn[a]	0.04	0.16	0.08	37.3	1.00	1.91	1.87	0.20
5 M Gdn[b]	0.07	0.07	0.10	2.05	1.13	1.82	1.65	0.50

[a]Emission wavelength, 330 nm. [b]Emission wavelength, 350 nm.

increase in the α-helix was not found in the partially unfolded state of β-momorcharin, the secondary structure remained more than 90%. These results demonstrate that β-momorcharin would unfold through a partially unfolded state similar to some other proteins. However, it should be noted that partially unfolded state of β-momorcharin exhibits a specific conformation at the vicinity of active site as shown in the experimental results on the detailed fluorescence studies on Trp-190.

The drastic difference in the fluorescence decay kinetics and its parameter was not found between the native and the partially unfolded states of β-momorcharin excited at 297 nm, although the average fluorescence lifetime at the native state was shorter a little suggesting the stronger interaction of Trp-190 with surrounding amino acid residues. On the excitation at 280 nm, the fluorescence decay kinetics of β-momorcharin gave a clear negative pre-exponential factor at the native and partially unfolded states. It doubtlessly shows that excitation energy transfer process involved in the fluorescence decay of tryptophan residue. As shown in Fig. 1, X-ray crystallographic structure reveals that Tyr-70 and Tyr-109 are arranged around the Trp-190. Based on the simple kinetic analysis, the fluorescence decay of the energy acceptor (tryptophan) is given by Eq. (5) where τ_D and τ_A are the fluorescence decay times of energy donor and acceptor, respectively, and k_t is the energy transfer rate and A_0 and D_0 are constant,

$$f(t) = \left[\frac{k_t D_0}{(1/\tau_A) - (1/\tau_D)}\right]\left[\exp\left(\frac{-t}{\tau_D}\right) - \exp\left(\frac{-t}{\tau_A}\right)\right] + A_0 \exp\left(\frac{-t}{\tau_A}\right) \quad (5)$$

In Eq. (5), the fluorescence lifetime of tyrosine residue is shorter, therefore, the inverse of decay time corresponding to the negative pre-exponential factor gives the energy transfer rate. According to Förster's resonance excitation energy transfer formalism, the distance (R) between tryptophan and tyrosine is estimated by the energy transfer efficiency (E) which is given by the experimentally determined τ_D through Eqs (6) and (7). The critical distance (R_0) is defined as the energy transfer distance where the energy transfer rate (k_t) is the same as the fluorescence decay rate of the energy donor.

$$E = k_t\ \tau_D = \frac{k_t}{k_t + (1/\tau_D^0)} \quad (6)$$

$$\frac{1}{E} - 1 = \left(\frac{R}{R_0}\right)^6 \quad (7)$$

When 14 Å and 3.27 ns were used as the critical distance and the fluorescence lifetime of the tyrosine residue in the absence of the energy acceptor to estimate the donor–acceptor distance, respectively (*22, 23*), the energy transfer rates were calculated to be 0.38/ns and 1.28/ns in the native and partially unfolded states of β-momorcharin. This increase in the transfer rate corresponds to the about 2 Å shrink of the distance between tryptophan and tyrosine residues in the peptide cage. The X-ray crystallographic structure shows the nearest neighboring tyrosine residue (Tyr-70) locates 8.61 Å apart from tryptophan residue. This value is shorter than the energy transfer distance obtained here for the native β-momorcharin (12.6 Å). The X-ray crystallographic structure also shows Tyr-109 is arranged near Trp-190. But the energy transfer rate corresponding to the distance between Trp-190 and Tyr-109 is estimated to be more than 3 times smaller than that of Trp-190-Tyr-70. Therefore, it is not unreasonable to consider that the working energy donor would be Tyr-70. Assuming that the same tyrosine residue contributes as the excitation energy donor, the distance between tryptophan and tyrosine shrink to 10.2 Å at the partially unfolded state. Such conformational change near the active site of β-momorcharin would be consistent with the fluorescence quenching results. The collisional quenching constant (k_q) was remarkably suppressed at the partially unfolded state as indicated in Table 2. This suggests that tryptophan residue flips to the hydrophobic core side of β-momorcharin to escape from the access of the quencher molecule leading to the contraction of Tyr-Trp distance.

Time-resolved fluorescence depolarization studies characterized well the feature of the partially unfolded state of β-momorcharin from the point of molecular dynamics. The fluorescence anisotropy decays of β-momorcharin were experimentally described with double exponential kinetics. They can be rearranged to Eq. (8), using the rotational freedom, the rotational correlation times for the tryptophyl segment, and the entire rotation of β-momorcharin, respectively.

$$r(t) = r_0\left\{f \exp\left(\frac{-t}{\phi_f}\right) + (1-f)\right\} \exp\left(\frac{-t}{\phi_p}\right) \quad (8)$$

The rotational correlation time of peptide element of tryptophan residue (ϕ_f), the entire rotational correlation time (ϕ_p), and the rotational freedom (f) are related with the experimentally decided β_1, β_2, ϕ_1 and ϕ_2 as,

$$\frac{1}{\phi_f} + \frac{1}{\phi_p} = \frac{1}{\phi_1}, \quad \phi_p = \phi_2, \quad f = \frac{\beta_1}{(\beta_1 + \beta_2)} \quad (9)$$

The rotational correlation time of peptide element including tryptophan is shorter at the partially unfolded

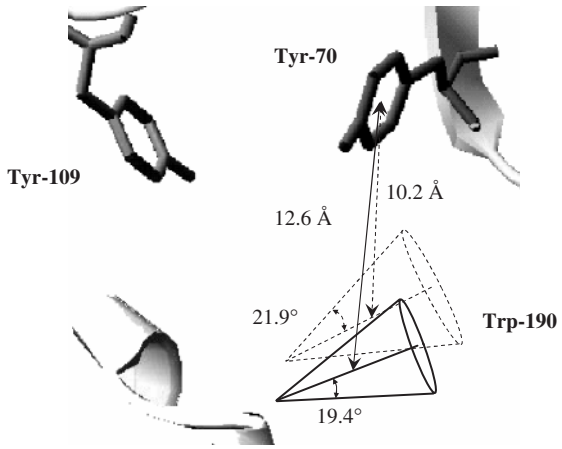

Fig. 9. **The anticipated changes in conformation and dynamics of β-momorcharin induced in the partially unfolded state.** The segmental motion of Trp-190 was represented with solid (native state) and dotted (partially unfolded state) cone. The distance between Trp-190 and Tyr-70 was drawn by the line between centers of Tyr-70 and the cone.

state than that at the native state. It suggests that the tryptophan fragment would be free from the stronger interactions with its surroundings. The motional freedom (f) is an interesting parameter to characterize the partially unfolded state of β-momorcharin and is represented by the semi-cone angle (θ) based on Eq. (10) (*24–26*).

$$(1-f)^{1/2} = \frac{1}{2}\cos\theta(\cos\theta + 1) \qquad (10)$$

The semi-cone angles of tryptophyl segment for the native and the partially unfolded states were estimated to be 19.4 and 21.9°, respectively.

The volume size of β-momorcharin increased, therefore, the whole structure would be relaxed in the partially unfolded state because the correlation time corresponding to the protein entire rotation was prolonged and the hydrophobic site was exposed to the surface. These are consistent with the nature of MG state generally known. But, the notable feature of partially unfolded state of β-momorcharin is the specific conformation near the active site. The anticipated conformation of the partially unfolded state of β-momorcharin is schematically figured out in Fig. 9. The motion of the peptide element including Trp-190 would be activated and it flips to the hydrophobic core site to shrink the distance between Tyr-70 and Trp-190. Hitherto, it is known that some proteins take such conformation that their Trp-motions are restricted before reaching their MG state (*27*). Although the partially unfolded state of β-momorcharin seems to have similar properties to Trp-restricted state because Trp residue is protected from the quencher molecule and its location is moved to the hydrophobic core side, it has more mobilized Trp-190 near the active site than in the native state.

REFERENCES

1. Anfinsen, C.B., Haber, E., Sela, M., and White, F.H. (1961) The kinetics of formation of native ribonuclease during oxidation of the reduced polypeptide chain. *Proc. Natl. Acad. Sci.* **47**, 1309–1314
2. Anfinsen, C.B. (1973) Principles that govern the folding of protein chains. *Science* **181**, 223–230
3. Kuwajima, K. (1989) The molten globule state as a clue for understanding the folding and cooperativity of globular-protein structure. *Proteins* **6**, 87–103
4. Radford, S.E., Dobson, C.M., and Evans, P.A. (1992) The folding of hen lysozyme involves partially structured intermediates and multiple pathways. *Nature* **358**, 302–307
5. Ptitsyn, O.B. (1995) Molten globule and protein folding. *Adv. Protein Chem.* **47**, 83–229
6. Arai, M. and Kuwajima, K. (2000) Role of the molten globule state in protein folding. *Adv. Protein Chem.* **53**, 209–282
7. Koshiba, T., Yao, M., Kobashigawa, Y., Demura, M., Nakagawa, A., Tanaka, I., Kuwajima, K., and Nitta, K. (2000) Structure and thermodynamics of the extraordinarily stable molten globule state of canine milk lysozyme. *Biochemistry* **39**, 3248–3257
8. Samuel, D., Kumar, T.K.S., Srimathi, T., Hsieh, H., and Yu, C. (2000) Identification and characterization of an equilibrium intermediate in the unfolding pathway of an all β-barrel protein. *J. Biol. Chem.* **275**, 34968–34975
9. Nitta, K. (2002) Alpha-lactalbumin and (calcium-binding) lysozyme. *Methods Mol. Biol.* **172**, 211–224
10. Schulman, B.A., Kim, P.S., Dobson, C.M., and Redfield, C. (1997) A residue-specific NMR view of the non-cooperative unfolding of a molten globule. *Nat. Struct. Biol.* **4**, 630–634
11. Kuznetsova, I.M., Turoverov, K.K., and Uversky, V.N. (2004) Use of the phase diagram method to analyze the protein unfolding-refolding reactions: fishing out the "invisible" intermediates. *J. Proteome. Res.* **3**, 485–494
12. Yuan, Y.R., He, Y.N., Xiong, J.P., and Xia, Z.X. (1999) Three-dimensional structure of beta-momorcharin at 2.55 Å resolution. *Acta Crystallogr. Sect.D* **55**, 1144–1151
13. Lakowicz, J.R. (1999) *Principles of Fluorescence Spectroscopy,* 2nd edn. Kluwer Academic/Plenum Publishers, New York
14. Fong, W.P., Poon, Y.T., Wong, T.M., Mock, J.W.Y., Ng, T.B., Wong, R.N.S., Yao, Q.Z., and Yeung, H.W. (1996) A highly efficient procedure for purifying the ribosome-inactivating proteins α- and β-momorcharins from *Momordica charantia* seeds. N-terminal sequence comparison and establishment of their *N*-glycosidase activity. *Life Science* **59**, 901–909
15. McKinnon, A.E., Szabo, A.G., and Miller, D.R. (1977) The deconvolution of photoluminescence data. *J. Phys. Chem.* **81**, 1564–1570
16. Uversky, V.N., Winter, S., and Löber, G. (1996) Use of fluorescence decay times of 8-ANS-protein complexes to study the conformational transitions in proteins which unfold through the molten globule state. *Biophys. Chem.* **60**, 79–88
17. Semisotnov, G.V., Rodionova, N.A., Kutyshenko, V.P., Ebert, B., Blanck, J., and Ptitsyn, O.B. (1987) Sequential mechanism of refolding of carbonic anhydrase B. *FEBS Lett.* **224**, 9–13
18. Semisotnov, G.V., Rodionova, N.A., Razgulyaev, O.I., Uversky, V.N., Gripas, A.F., and Gilmanshin, R.I. (1991) Study of the "molten globule" intermediate state in protein folding by a hydrophobic fluorescent probe. *Biopolymers* **31**, 119–128
19. Kuwajima, K., Nitta, K., and Sugai, S. (1975) Electrophoretic investigations of the acid conformational change of α-lactalbumin. *J. Biochem.* **78**, 205–211
20. Morozova-Roche, L.A., Arico-Muendel, C.C., Haynie, D.T., Emelyanenko, V.I., Dael, H.V., and Dobson, C.M. (1997)

Structural characterization and comparison of the native and A-states of equine lysozyme. *J. Mol. Biol.* **268**, 903–921
21. Watanabe, M., Kobashigawa, Y., Aizawa, T., Demura, M., and Nitta, K. (2004) A non-native α-helix is formed in the β-sheet region of the molten globule state of canine milk lysozyme. *Protein J.* **23**, 335–342
22. Eisinger, J., Feuer, B., and Lamola, A.A. (1969) Intramolecular singlet excitation transfer. Applications to polypeptides. *Biochemistry* **8**, 3908–3915
23. Oishi, O., Yamashita, S., Nishimoto, E., Lee, S., Sugihara, G., and Ohno, M. (1997) Conformations and orientations of aromatic amino acid residues of tachyplesin I in phospholipid membranes. *Biochemistry* **36**, 4352–4359
24. Lipari, G. and Szabo, A. (1982) Model-free approach to the interpretation of nuclear magnetic resonance relaxation in macromolecules. 2. Analysis of experimental results. *J. Am. Chem. Soc.* **104**, 4559–4570
25. Chen, R.F., Knutson, J.R., Ziffer, H., and Porter, D. (1991) Fluorescence of tryptophan dipeptides: correlations with the rotamer model. *Biochemistry* **30**, 5184–5195
26. Nishimoto, E., Yamashita, S., Szabo, A.G., and Imoto, T. (1998) Internal motion of lysozyme studied by time-resolved fluorescence depolarization of tryptophan residues. *Biochemistry* **37**, 5599–5607
27. Kuznetsova, I.M., Stepanenko, O.V., Turoverov, K.K., Zhu, L., Zhou, J-M., Fink, A.L., and Uversky, V.N. (2002) Unraveling multistate unfolding of rabbit muscle creatine kinase. *Biochim. Biophys. Acta.* **1596**, 138–155